



ELSEVIER

12 October 2000

Physics Letters B 491 (2000) 8–14

PHYSICS LETTERS B

www.elsevier.nl/locate/npe

Low-lying intruder 1^- state in ^{12}Be and the melting of the $N = 8$ shell closure

H. Iwasaki^{a,*}, T. Motobayashi^b, H. Akiyoshi^c, Y. Ando^b, N. Fukuda^a, H. Fujiwara^b,
Zs. Fülöp^{c,1}, K.I. Hahn^{c,2}, Y. Higurashi^b, M. Hirai^a, I. Hisanaga^b, N. Iwasa^c,
T. Kijima^b, A. Mengoni^{c,d}, T. Minemura^b, T. Nakamura^a, M. Notani^c, S. Ozawa^b,
H. Sagawa^e, H. Sakurai^c, S. Shimoura^b, S. Takeuchi^b, T. Teranishi^c, Y. Yanagisawa^b,
M. Ishihara^{a,c}

^a Department of Physics, University of Tokyo, 7-3-1 Hongo, Bunkyo, Tokyo 113-0033, Japan

^b Department of Physics, Rikkyo University, 3-34-1 Nishi-Ikebukuro, Toshima, Tokyo 171-8501, Japan

^c The Institute of Physical and Chemical Research (RIKEN), 2-1 Hirosawa, Wako, Saitama 351-0198, Japan

^d ENEA, Applied Physics Division, Via Don Fiammelli 2, I-40129 Bologna, Italy

^e Center for Mathematical Sciences, the University of Aizu, Aizu-Wakamatsu, Fukushima 965-8580, Japan

Received 29 June 2000; received in revised form 28 August 2000; accepted 28 August 2000

Editor: J.P. Schiffer

Abstract

Inelastic scattering of the neutron-rich nucleus ^{12}Be on lead and carbon targets has been studied by measuring de-excitation γ rays in coincidence with scattered ^{12}Be . The strong γ -ray transition from the state at $E_x = 2.68(3)$ MeV following E1 Coulomb excitation was observed for the lead target, leading to an assignment of $J^\pi = 1^-$ for the excited state. The low excitation energy of this intruder 1^- state and the deduced large $B(E1; 0_{g.s.}^+ \rightarrow 1^-)$ value of $0.051(13)e^2 \text{ fm}^2$ provide a consistent picture of the $N = 8$ shell melting in ^{12}Be . © 2000 Elsevier Science B.V. All rights reserved.

PACS: 25.70.De; 25.60.-t; 23.20.-g; 27.20.+n

The electric dipole (E1) strength in a nucleus is largely exhausted by a giant dipole resonance, which is constructed from a superposition of many particle–hole excitations, and essentially no E1 strength appears in low energy region below 5 MeV. It is not the

case for some of light nuclei. In particular, a strong E1 strength is expected if the low-lying intruder positive parity state appears close to the negative parity states. The transition between the first excited $\frac{1}{2}^-$ state at $E_x = 0.32$ MeV and the $\frac{1}{2}^+$ ground state in ^{11}Be is a well-known example of this anomaly, representing one of the strongest E1 transitions ever observed between nuclear bound levels [1]. Such a favoured E1 transition may be induced by a decoupled feature of the valence neutron and an extended single-particle wave function of one neutron halo in these two loosely

* Corresponding author.

E-mail address: iwasaki@rarfaxp.riken.go.jp (H. Iwasaki).

¹ On leave from ATOMKI, Debrecen, Hungary.

² Present address: Department of Science Education, Ewha Woman's University, Seoul 120-750, Korea.

bound states. The measurement of the low-lying E1 strength has been extended to the continuum excitation of loosely bound neutron-rich nuclei ^{11}Li [2–4] and ^{11}Be [5], where halo neutrons also play an essential role to increase the strength.

Recently, the ^{12}Be nucleus obtains much attention because of the possible shell melting in the $N = 8$ isotones [6–8]. An evidence of disappearance of magicity in ^{12}Be has been obtained by our earlier study of proton inelastic scattering on ^{12}Be [7]. A knockout reaction of ^{12}Be measured at MSU also showed a strong indication of the shell melting in its ground state [8]. It is expected that the resultant smaller gap between p -shell and sd -shell brings down the lowest 1^- state considerably. A unique feature of ^{12}Be is possible strong correlations of two neutrons outside the core in the ground state. These correlations may cause a coherent effect in the transition amplitudes and help to enhance the low energy E1 strength substantially [9].

Experimentally, an attempt has been made to search for the low-lying 1^- state in ^{12}Be and an upper limit has been obtained for the E1 strength in the energy range from 0.15 MeV to 2.00 MeV [10]. The candidate of such a state has been observed in the neighboring isotone ^{11}Li [2–4,11,12], though the experimental accuracy and the theoretical interpretation of the E1 strength are still controversial because the observed E1 strength is above the threshold [13,14]. Since ^{12}Be has a higher neutron threshold energy at 3.17 MeV, it is probable that the 1^- state appears as a discrete bound state. Thus a further experiment to find the 1^- state is strongly encouraged.

In the present experiment, we have studied inelastic scattering of ^{12}Be on lead ($Z = 82$) and carbon ($Z = 6$) targets at intermediate energies of about 50 MeV/u. Comparison of the cross section between the high- Z and low- Z targets provides a tool to distinguish between the E1 ($l = 1$) and E2 ($l = 2$) excitations. While the Coulomb excitation cross section sharply rises with increasing target Z , the relative importance between the Coulomb and nuclear contributions varies with the transition multipolarity. For an unhindered E1 transition, the Coulomb contribution dominates over the nuclear contribution for a high- Z target, whereas only a small cross section due to the nuclear interaction is left for a low- Z target. For the case of E2 excitation, the nuclear contribution becomes more significant and may become compatible with

the Coulomb contribution even with a heavy target such as lead. By exploiting these features, the inelastic scattering incorporating a combination of heavy and light targets has provided a useful means to populate and identify the 1^- state in ^{12}Be .

The experiment was carried out at the RIKEN Accelerator Research Facility using the same experimental arrangement described in Ref. [7]. We measured de-excitation γ rays in coincidence with inelastically scattered particles. Angle-integrated cross sections were deduced from the observed γ -ray yields. A radioactive ^{12}Be beam was produced by the fragment separator RIPS [15] via fragmentation reactions of a 100 MeV/u ^{18}O primary beam on a 1.11 g/cm² ^9Be target. Two 1 mm thick plastic scintillators placed 5.3 m apart along the beam line were used to identify secondary beam particles on an event-by-event basis. The resulting beam of ^{12}Be had a typical intensity of 2×10^4 counts per second. The isotopic purity was found to be around 96%. The ^{12}Be beam bombarded a secondary target placed at the final focal plane of RIPS. Two different targets (350.8 mg/cm² thick ^{208}Pb and 89.8 mg/cm² thick ^{12}C) were used to excite the projectiles. The beam energies in the middle of the targets were calculated to be 53.3 MeV/u and 54.0 MeV/u, respectively, for the lead and carbon targets. A measurement with the target removed was also made to evaluate background contributions.

After passing through the secondary target, scattered particles were stopped in a ΔE - E plastic scintillator hodoscope (details are given in Ref. [7]) located downstream of the secondary target. The isotopic identification of the scattered particles was performed by the time-of-flight(TOF)- ΔE and TOF- E methods. The hodoscope with a total active area of $1 \times 1 \text{ m}^2$ had a finite acceptance up to 6.8 degrees. This angle corresponds to $\theta_{\text{cm}} = 7.3^\circ$ for the lead target and $\theta_{\text{cm}} = 13.9^\circ$ for the carbon target. In the present study, we have deduced the angle-integrated cross sections, defined as $\sigma_{\text{Pb}}(\theta_{\text{cm}} \leq 7.3^\circ)$ and $\sigma_{\text{C}}(\theta_{\text{cm}} \leq 13.9^\circ)$ for the respective targets. The overall efficiencies of the hodoscope relevant to the angle-integrated cross sections were estimated by a Monte Carlo simulation, which took into account the finite size and angular spread of the incident beam, the multiple scattering in the secondary targets (0.5 degrees and 0.1 degrees in r.m.s., respectively, for the lead and carbon targets), and the detector geometry. Theoretical angular distri-

butions calculated with the ECIS79 code [16] were incorporated in this simulation to properly evaluate the effective angular acceptance of the hodoscope. The calculated overall efficiencies were about 80%.

Fifty-five NaI(Tl) detectors surrounding the target were used to detect the de-excitation γ rays. The intrinsic energy resolution of each detector was typically 7.0% (FWHM) for the 1275-keV γ ray. The absolute efficiency and the line shape of the γ -ray energy spectrum were simulated by means of a GEANT code [17]. The total photo-peak efficiencies were calculated to be 7.1% and 5.7%, respectively, for 2.11-MeV and 2.68-MeV γ rays emitted from a ^{12}Be nucleus moving with $v/c \approx 0.3$. The simulated spectral shape of a γ ray was used as a fitting function in deducing a photo-peak yield from the experimental energy spectrum.

Fig. 1 shows the Doppler-corrected γ -ray energy spectra measured in coincidence with scattered ^{12}Be isotopes. In the figure, the de-excitation γ rays, corresponding to the previously known $2_1^+ \rightarrow 0_{g.s.}^+$ transition in ^{12}Be , are evident at 2.11(2) MeV for both the lead and carbon targets. Another peak is clearly observed at 2.68(3) MeV for the lead target, whereas no significant peak is observed for the carbon target. This yield dependence on the target indicates the dominance of the Coulomb contribution for the 2.68-MeV γ rays. Since only two bound states (2.10 MeV and 2.70 MeV [18]) have ever been known in ^{12}Be , it is likely that the 2.68-MeV peak corresponds to the transition from the second excited state to the ground state. The second excited state of ^{12}Be has been observed in the vicinity of 2.70 MeV in several reactions such as $^{14}\text{C}(^{14}\text{C}, ^{12}\text{Be})^{16}\text{O}$ [19] and $^{10}\text{Be}(t, p)^{12}\text{Be}$ [20], while no clear J^π assignment is given. Occurrence of the γ transition as observed in the present measurement excludes the possibility of the $J^\pi = 0^+$ assignment discussed in Ref. [19,20].

In the present study, the measurement was also performed with a 60.0 MeV/u ^{10}Be secondary beam incident on the lead target. This was made to evaluate the contribution from the ^{208}Pb excitation leading to the 3_1^- state at 2.61 MeV, which is rather close to the observed γ -ray energy of 2.68 MeV. The $^{10}\text{Be} + ^{208}\text{Pb}$ inelastic scattering provided useful information on the magnitude of the ^{208}Pb excitation, since it is almost identical with that for the ^{12}Be reaction, while the γ -ray peaks of ^{10}Be (such as the 3.37-MeV peak of the 2_1^+ state) are more separate from

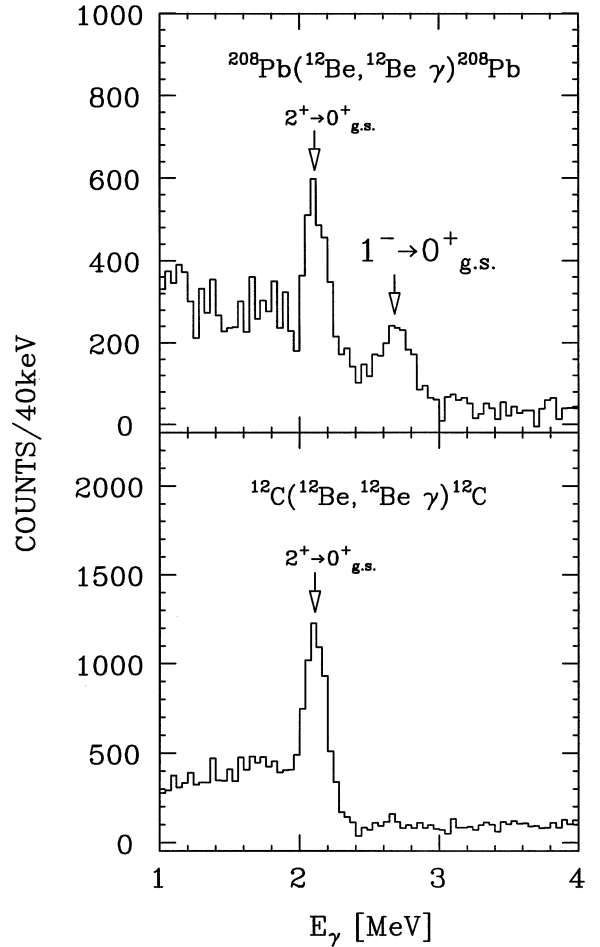


Fig. 1. Doppler-corrected γ -ray energy spectra measured in the inelastic scattering of ^{12}Be on the lead (top) and carbon (bottom) targets.

the ^{208}Pb peak. Fig. 2 (right) shows γ -ray energy spectra measured in coincidence with scattered ^{10}Be isotopes. In the observed γ -ray spectrum without any Doppler correction (Fig. 2(b)), a clear peak can be seen around 2.61 MeV, showing that the ^{208}Pb excitation indeed occurred. In contrast, the relevant events are widely distributed in the Doppler-corrected energy spectrum obtained with respect to the projectile frame of ^{10}Be (Fig. 2(d)). When the data from the NaI(Tl) detectors placed at around 90° were used, the Doppler-corrected spectrum yielded a peak around 2.76 MeV corresponding to the ^{208}Pb γ transition. On the other hand, the ^{208}Pb peaks were apart from either of the

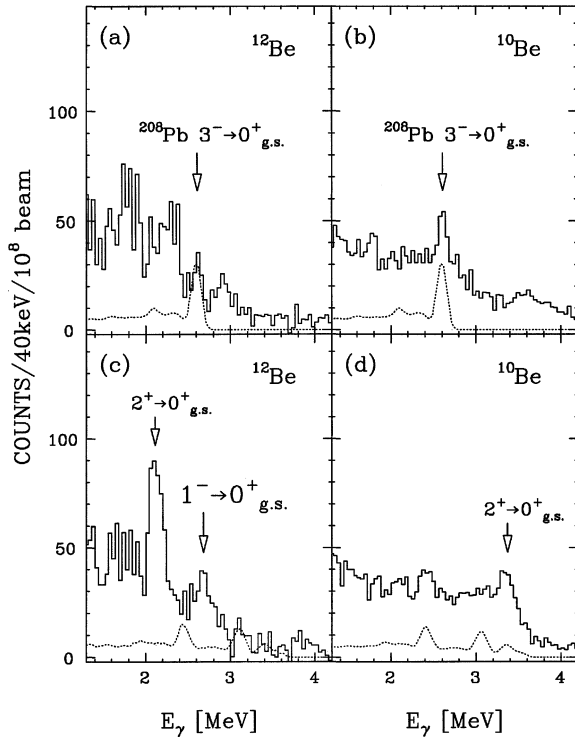


Fig. 2. Left (right) panels show γ -ray energy spectra measured in the ^{12}Be (^{10}Be) + ^{208}Pb inelastic scattering. The spectra are normalized by the total number of incident particles. Top (bottom) panels contain spectra obtained in the laboratory (projectile) frame. The dotted curves represent simulated spectra for the 2.61-MeV ^{208}Pb transition. In these spectra (a)–(d), the data from the 90° detectors are excluded (see text).

two peaks from the ^{12}Be excitation as far as the data with the other NaI(Tl) detectors were used. In the final analysis for ^{12}Be , we therefore excluded the data from the 90° detectors and obtained the spectra shown in Fig. 2 (left). The 2.61-MeV peak is also clearly seen in the laboratory frame spectrum (Fig. 2(a)). As confirmed in the case of ^{10}Be , the ^{208}Pb peak should not make any significant contribution to the energy region around 2.68 MeV in the Doppler-corrected spectrum of ^{12}Be . Nevertheless, the spectrum shown in Fig. 2(c) clearly exhibits a peak at 2.68 MeV, verifying the assignment that the γ transition belongs to ^{12}Be .

The angle-integrated cross sections for the inelastic scattering were obtained from measured γ -ray yields after correcting for the detection efficiencies of both γ rays and scattered particles. The angular distribu-

Table 1

Experimental angle-integrated cross sections for the inelastic scattering of ^{12}Be on the lead and carbon targets. The $J^\pi = 1^-$ assignment for the state at $E_x = 2.68(3)$ MeV is determined by the present work. The 1σ upper limit is presented for the 1^- excitation by the carbon target

J^π	E_x [MeV]	$\sigma_{\text{Pb}}(\theta_{\text{cm}} \leq 7.3^\circ)$ [mb]	$\sigma_{\text{C}}(\theta_{\text{cm}} \leq 13.9^\circ)$ [mb]
1^-	2.68(3)	46.5(11.5)	< 4.9
2^+	2.11(2)	81.8(12.8)	54.9(7.1)

tion of the inelastic scattering was calculated by the ECIS code to be incorporated in the efficiency simulation as well as to deduce the transition strength as discussed later. For the $^{12}\text{Be} + ^{208}\text{Pb}$ scattering, we took the optical potential parameters as obtained by the $^{17}\text{O} + ^{208}\text{Pb}$ scattering at 84 MeV/u [21], while for the $^{12}\text{Be} + ^{12}\text{C}$ scattering, we used the potential parameters determined by the $^{12}\text{Be} + ^{12}\text{C}$ scattering measured at 57 MeV/u [22]. The nuclear contribution was evaluated by assuming a simple collective vibration mode with $\delta = \delta^N = \delta^C$, where δ^N and δ^C denote the nuclear and Coulomb deformation lengths. The uncertainty of the calculated efficiency arising from the theoretical angular distribution is negligible, as far as the transition multipolarity was taken among E1 (M1) or E2. This was because of the large dimension of the hodoscope. Note that the excitation via higher multipolarity is expected to be negligibly weak. Thus, for the purpose of the efficiency simulation, we safely assumed E1 multipolarity of the transition to the second excited state, while E2 multipolarity was obviously employed for the first excited state of 2_1^+ .

Table 1 shows the deduced angle-integrated cross sections. In deducing these cross sections, the photopeak yields were extracted after subtracting the estimated contributions from the ^{208}Pb excitation. This was made using the simulated spectra for the 2.61-MeV ^{208}Pb transition as shown by dotted curves in Fig. 2, which were calculated to match the data on ^{10}Be . The cross section σ_{Pb} of 46.5(11.5) mb was thus obtained for the 2.68-MeV peak of ^{12}Be . The quoted error includes ambiguities in the photo-peak yield (21%), the hodoscope efficiency (5%), and the γ -ray detection efficiency (10%). Though no significant peak of the second excited state was observed for the carbon target, we could place the 1σ upper limit of

4.9 mb on σ_C . The results of the angle-integrated cross sections exciting the 2_1^+ state are also summarized in Table 1.

We first discuss the spin and parity of the second excited state of ^{12}Be , since they have not ever been clearly assigned. As noted before, the excitation to the second excited state is dominated by the Coulomb contribution. Consequently, the electromagnetic transition strength can be readily deduced from the experimental cross section if a certain multipolarity is assumed, and the spin and parity of the 2.68-MeV state are constrained as follows. Utilizing the equivalent photon method based on the first order perturbation theory [23], the corresponding γ -decay strength was extracted from the experimental cross section 46.5 mb to be 0.050 Weisskopf units (W.u.), 11 W.u., and 11 W.u., respectively, for the cases of E1, M1, and E2 transitions. From the compilation of the experimental data in this mass region [24], a value of 11 W.u. for a M1 transition is too large and hence the $J^\pi = 1^+$ assignment can be excluded. Thus the remaining possibility is $J^\pi = 1^-$ (E1) or $J^\pi = 2^+$ (E2).

For inelastic scattering with a heavy target like lead, the Coulomb dominance of the E1 excitation has been proved both experimentally [25] and theoretically [26, 27], while the dominance becomes much weaker in the case of E2 transition of light projectiles [28]. Thus the observed Coulomb dominance already suggests E1 nature of the 2.68-MeV transition and hence the 1^- assignment for the second excited state. This conclusion is further substantiated by the ECIS calculation. The deformation length δ was translated from the measured cross section with the lead target. In the calculation, the deformation length was taken to be the same for the Coulomb and nuclear potentials. The results of δ were 0.24 fm and 1.56 fm, respectively, for the E1 and E2 cases. Using these deformation lengths, we estimated the cross sections with the carbon target. The results were 1.1 mb for E1 and 33.8 mb for E2. The experimental upper limit of the cross section, 4.9 mb, can only be explained by the E1 transition. It should be noted that the E1 cross section for carbon may be even smaller than the above quoted value (1.1 mb) due to the iso-scalar nature of the nuclear excitation induced by ^{12}C .

The significant nuclear contribution to the E2 transition as expected above can be quantitatively shown by the ECIS analysis of the 2_1^+ excitation. By assum-

ing $\delta = \delta^N = \delta^C$, the deformation lengths were deduced to be 2.04(16) fm and 1.93(11) fm, respectively, for the data with the lead and carbon targets. Note that both these values are consistent with the result of 2.00(23) fm obtained by our earlier study on the proton inelastic scattering [7]. In these calculations, the nuclear excitation contribution yields 80.3 mb and 57.3 mb, respectively, for σ_{pb} and σ_C , demonstrating that the observed cross sections for both of the targets (81.8 mb and 54.9 mb) are dominated by the nuclear excitation.

Based on the above discussion, we conclude that the excitation to the second excited state occurred via an E1 transition. The spin and parity of the state is then determined to be 1^- uniquely. The E1 strength is obtained to be $B(E1; 0_{\text{g.s.}}^+ \rightarrow 1^-) = 0.051(13)e^2\text{fm}^2$ by the ECIS calculation.

The location of the lowest 1^- state provides a useful measure of the energy difference between the $1p_{1/2}$ and $2s_{1/2}$ orbitals, $\Delta\epsilon = \epsilon(\frac{1}{2}^+) - \epsilon(\frac{1}{2}^-)$, since the main configuration of the 1^- state is expected to be the excitation between $1p_{1/2}$ and $2s_{1/2}$ states in a naive single particle picture. Comparison of the excitation energies of the 1^- state, $E_x(1^-)$, among $N = 8$ isotones ($^{16}\text{O} : 7.12$ MeV, $^{14}\text{C} : 6.09$ MeV, $^{12}\text{Be} : 2.68$ MeV) depicts the sharp decrease of $E_x(1^-)$ at the Be

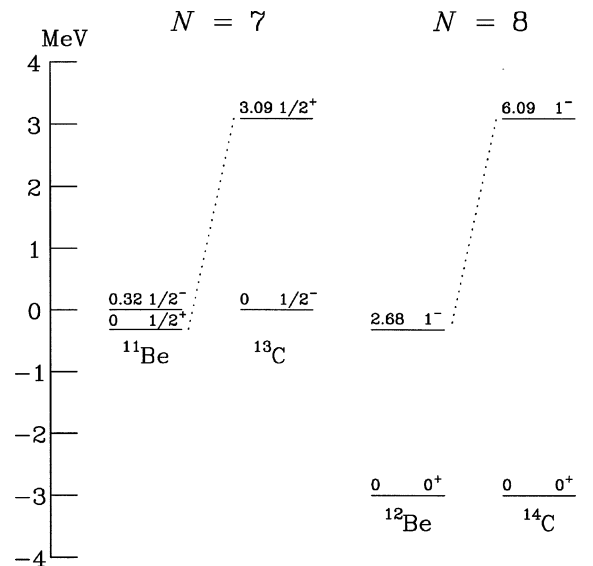


Fig. 3. Energy levels in the Be and C isotopes with the neutron number $N = 7$ [29] and $N = 8$.

isotone, indicating the drastic narrowing of the shell gap at ^{12}Be . In Fig. 3, the relevant energy levels are compared between the Be and C isotopes with $N = 7$ and $N = 8$. When one moves from ^{13}C to ^{11}Be , $\Delta\epsilon$ drops by about 3.4 MeV. A near degeneracy of the $2s_{1/2}$ and $1p_{1/2}$ orbitals achieved at ^{11}Be represents the $N = 8$ shell melting [29]. Similarly, $E_x(1^-)$ decreases from ^{14}C to ^{12}Be . Incidentally the magnitude of the lowering of $E_x(1^-)$ is almost identical with that of $\Delta\epsilon$ in the $N = 7$ isotones. This observation strongly supports that the degeneracy of the two orbitals is promoted in ^{12}Be as well as in ^{11}Be . Recently the same trend of the anomalous reduction of $\Delta\epsilon$ was found for the $N = 9$ nucleus ^{14}B in the β -decay study of ^{14}Be [30]. Thus, one can conclude that the $N=8$ shell melting is a general phenomenon which occurs widely in the neutron-rich nuclei around ^{12}Be .

Finally, we discuss the E1 strength, $B(\text{E}1) = 0.051(13)e^2\text{fm}^2$, obtained for the $0_{\text{g.s.}}^+ \rightarrow 1^-$ transition, which is the first example of strong low-lying E1 transition observed in even–even nuclei. In groping for a possible enhancement mechanism, we refer to the prescription of the E1 doorway state [9]. Firstly, the ^{12}Be ground state is considered as a ^{10}Be core and correlated two neutrons moving outside the core,

$$|^{12}\text{Be}:0^+\rangle = \alpha|(1p_{1/2})^2\rangle + \beta|(2s_{1/2})^2\rangle. \quad (1)$$

In the limit of the complete degeneracy of the two orbitals, we have the amplitudes $\alpha = \beta = 1/\sqrt{2}$. Then a coherent 1^- excitation of the correlated two neutrons [9] is written as a doorway state for the dipole operator

$$\begin{aligned} \hat{O}_\mu^{\lambda=1} &= \sum_{i=1}^N \frac{Z}{A} r_i Y_{1\mu}(r_i) - \sum_{i=1}^Z \frac{N}{A} r_i Y_{1\mu}(r_i); \\ |^{12}\text{Be}:1^-\rangle &= \frac{1}{N} \hat{O}^{\lambda=1} |^{12}\text{Be}:0^+\rangle \\ &= 0.63|(2s_{1/2}1p_{1/2}^{-1})\rangle \\ &\quad + 0.63|(1p_{1/2}2s_{1/2}^{-1})\rangle \\ &\quad + 0.45|(2s_{1/2}1p_{3/2}^{-1})\rangle, \end{aligned} \quad (2)$$

where N is a normalization constant, and the coefficients are proportional to the single particle matrix elements of the dipole operator $\hat{O}^{\lambda=1}$. In this equation, the particle–hole excitations are limited to the configuration space of p, s orbitals to highlight coherent con-

tributions of these excitations. The coefficients are obtained taking into account the small separation energies of the $1p_{1/2}$ and $2s_{1/2}$ states in ^{12}Be . The $B(\text{E}1)$ value between the two states (1) and (2) is expressed as

$$\begin{aligned} B(\text{E}1; 0^+ \rightarrow 1^-) &= |(1^- || \hat{O}^{\lambda=1} || 0^+)|^2 \\ &= |0.63\langle 2s_{1/2} || \hat{O}^{\lambda=1} || 1p_{1/2} \rangle \\ &\quad + 0.63\langle 1p_{1/2} || \hat{O}^{\lambda=1} || 2s_{1/2} \rangle \\ &\quad + 0.45\langle 2s_{1/2} || \hat{O}^{\lambda=1} || 1p_{3/2} \rangle|^2. \end{aligned} \quad (3)$$

We can see in Eq. (3) that the degeneracy of $1p_{1/2}$ and $2s_{1/2}$ states indeed enhances the $B(\text{E}1)$ value about twice more than the single-particle transition rate

$$|\langle 2s_{1/2} || \hat{O}^{\lambda=1} || 1p_{1/2} \rangle|^2.$$

To make a more quantitative study, a shell model calculation involving a larger configuration space is desirable.

There has been so far one theoretical attempt to describe the low-lying 1^- state in ^{12}Be [31]. This work, which is based on a two-neutron pairing model [32], has predicted the lowest 1^- state in ^{12}Be at 2.7 MeV with a somewhat larger $B(\text{E}1)$ value of $0.23e^2\text{fm}^2$. They also pointed out that the strong correlation between the $(1p_{1/2})^2$ and $(2s_{1/2})^2$ configurations enhances the E1 strength. The deviation of the calculated $B(\text{E}1)$ value from the present experimental result might be attributed to the extended wave function adopted for the calculation.

In conclusion, we have studied inelastic scattering of the ^{12}Be nucleus using lead and carbon targets. The spin-parity assignment $J^\pi = 1^-$ for the state at 2.68(3) MeV explains successfully the experimental cross sections of the two targets, excluding other possible spin-parity assignments. The large $B(\text{E}1; 0_{\text{g.s.}}^+ \rightarrow 1^-)$ value of $0.051(13)e^2\text{fm}^2$ for the 2.68-MeV state was deduced. The lowering of the intruder 1^- state accompanied with the large E1 strength represents the characteristic feature of degenerate $1p_{1/2}$ and $2s_{1/2}$ states, thus indicating the melting of $N = 8$ magicity in ^{12}Be .

Acknowledgements

Sincere gratitude is extended to the staff members of the RIKEN Ring Cyclotron for their operation of

the accelerator during the experiment. The present work is supported in part by the Ministry of Education, Science, Sports and Culture by Grant-In-Aid for Scientific Research under the program number (B) 08454069.

References

- [1] D.J. Millener et al., *Phys. Rev. C* 28 (1983) 497.
- [2] K. Ieki et al., *Phys. Rev. Lett.* 70 (1993) 730;
D. Sackett et al., *Phys. Rev. C* 48 (1993) 118.
- [3] S. Shimoura et al., *Phys. Lett. B* 348 (1995) 29.
- [4] M. Zinser et al., *Nucl. Phys. A* 619 (1997) 151.
- [5] T. Nakamura et al., *Phys. Lett. B* 331 (1994) 296.
- [6] Toshio Suzuki, Takaharu Otsuka, *Phys. Rev. C* 56 (1997) 847.
- [7] H. Iwasaki et al., *Phys. Lett. B* 481 (2000) 7.
- [8] A. Navin et al., *Phys. Rev. Lett.* 85 (2000) 266.
- [9] Toshio Suzuki, H. Sagawa, P.F. Bortignon, *Nucl. Phys. A* 662 (2000) 282.
- [10] R. Anne et al., *Z. Phys. A* 352 (1995) 397.
- [11] T. Kobayashi, *Nucl. Phys. A* 538 (1992) 343c.
- [12] A.A. Korshennikov et al., *Phys. Rev. Lett.* 78 (1997) 2317.
- [13] H. Sagawa et al., *Z. Phys. A* 351 (1995) 385.
- [14] S. Karataglidis et al., *Phys. Rev. Lett.* 79 (1997) 1447.
- [15] T. Kubo et al., *Nucl. Instrum. Methods Phys. Res. B* 70 (1992) 309.
- [16] J. Raynal, Coupled channel code ECIS79, unpublished.
- [17] CERN Program library Long Writeup, W5013.
- [18] F. Ajzenberg-Selove, *Nucl. Phys. A* 506 (1990) 1.
- [19] M. Bernas, J.C. Peng, N. Stein, *Phys. Lett. B* 116 (1982) 7.
- [20] H.T. Fortune, G.-B. Liu, D.E. Alburger, *Phys. Rev. C* 50 (1994) 1355.
- [21] J. Barrette et al., *Phys. Lett. B* 209 (1988) 182.
- [22] M. Zahar et al., *Phys. Rev. C* 49 (1994) 1540.
- [23] C.A. Bertulani, G. Baur, *Phys. Rep.* 163 (1988) 299.
- [24] P.M. Endt, *At. Data Nucl. Data Tables* 23 (1979) 3.
- [25] M. Frauerbach et al., *Phys. Rev. C* 56 (1997) R1.
- [26] T. Motobayashi et al., *Phys. Lett. B* 264 (1991) 259.
- [27] C.A. Bertulani, *Phys. Rev. C* 49 (1994) 2688.
- [28] T. Motobayashi, in: H. Utsunomiya, M. Ohta, J. Galin, G. Münzenberg (Eds.), *Proc. Tours Symposium on Nuclear Physics II*, Tours, France, World Scientific, Singapore, 1994, p. 61.
- [29] I. Talmi, I. Unna, *Phys. Rev. Lett.* 4 (1960) 469.
- [30] N. Aoi et al., *Nucl. Phys. A* 616 (1997) 181c.
- [31] A. Bonaccorso, N. Vinh Mau, *Nucl. Phys. A* 615 (1997) 245.
- [32] N. Vinh Mau, J.C. Pacheco, *Nucl. Phys. A* 607 (1996) 163.